Supplementary Material (ESI) for Soft Matter

Supporting Information to:

Nanoobjects coming from mesomorphic ionic PAMAM dendrimers

Silvia Hernández-Ainsa[a], Joaquín Barberá[a], Mercedes Marcos[a], José Luis Serrano*[b]

[a]Departamento de Química Orgánica, Facultad de Ciencias-Instituto de Ciencia de Materiales de Aragón, Universidad de Zaragoza-CSIC, C/ Pedro Cerbuna 12, 50009-Zaragoza (Spain).

[b]Departamento de Química Orgánica, Instituto de Nanociencia de Aragón, Universidad de Zaragoza, Pedro Cerbuna 12, 50009-Zaragoza (Spain). joseluis@unizar.es

Table of Contents

1. Synthesis and characterization of the ionic dendrimers.
    1.1. Typical procedure for the synthesis of the ionic dendrimers
    1.2. FT-IR and NMR data of the ionic dendrimers.
2. Thermogravimetric data.
3. POM textures of the compounds.
4. Phase transition temperatures.
5. X-ray data
    5.1. Structural parameters of the columnar rectangular mesophase.
    5.2. X-ray diffractogrammes
6. Turbidity curves by water addition.
7. AFM images
8. TEM images
9. Rhodamine B and β-carotene encapsulation procedures.

1. Synthesis and Characterization of the ionic dendrimers.

1.1. Typical procedure for the synthesis of the ionic dendrimers

The ionic complexes were prepared by addition of a solution in dry tetrahydrofuran (THF) containing the fatty acid to a solution of THF containing PAMAM (approx 150 mg). The acid was added in the stoichometry necessary to functionalize all the amine groups of the PAMAM, namely “2n-2” , being “n” the primary amine groups and “n-2” the tertiary amine groups (the values of “n” depend on the generation and they are gathered in Scheme 1 of the main text). The mixture was ultrasonicated for 5 min, and then it was slowly evaporated at room temperature and dried in vacuum at 40 °C until the weight remained constant for approx 12 h. All of the resulting compounds present good solubility in ethanol, dichloromethane and chloroform.

1.2. FT-IR and NMR data of the ionic dendrimers.

G0(C_{14}): (as example of the serie G0(C_m))

^{1}H-RMN (400 MHz, $CDCl_3$): δ= 9.00-8.50 ($CON\underline{H}$), 6.20-5.80 ($N\underline{H}^+CH_2CH_2N$, $NHCH_2CH_2N\underline{H}_3^+$, $NHCH_2CH_2N\underline{H}^+$), 3.50-3.32 ($NHC\underline{H}_2CH_2NH_3^+$), 3.28-3.15 ($NH^+C\underline{H}_2CH_2N$,$NH^+C\underline{H}_2CH_2NH^+$), 3.14-2.98 ($NH^+C\underline{H}_2CH_2CONH$, $NHCH_2C\underline{H}_2NH_3^+$), 2.78-2.65 ($NC\underline{H}_2CH_2CONH$, $NH^+CH_2C\underline{H}_2N$), 2.62-2.52 ($NC\underline{H}_2CH_2N$), 2.52-2.45 ($NH^+CH_2C\underline{H}_2CONH$), 2.40-2.28 ($NCH_2C\underline{H}_2CONH$), 2.15 (t, J=7.7Hz, $CH_2C\underline{H}_2COO^-$), 1.53-1.49 ($C\underline{H}_2CH_2COO^-$), 1.32-1.28 ($CH_3(C\underline{H}_2)_x$), 0.87 (t, J=6.9Hz,$C\underline{H}_3CH_2$). ^{13}C-RMN (400 MHz, $CDCl_3$): δ= 180.5 ($\underline{C}OO^-$), 173.2-172.0 ($\underline{C}ONH$), 49.9 ($N\underline{C}H_2CH_2CONH$), 48.4 ($NC\underline{H}_2CH_2N$, $NC\underline{H}_2CH_2NH^+$), 44.1 ($NH^+C\underline{H}_2CH_2CONH$), 43.8 ($NH^+C\underline{H}_2CH_2N$), 39.4-38.4 ($NHCH_2\underline{C}H_2NH_3^+$,$NHCH_2C\underline{H}_2NH^+$), 37.4-37.2 ($NH\underline{C}H_2CH_2NH^+$, $NH\underline{C}H_2CH_2NH_3^+$), 36.9 ($CH_2\underline{C}H_2COO^-$), 33.9 ($NCH_2\underline{C}H_2CONH$), 32.2 ($NH^+CH_2C\underline{H}_2CONH$), 31.9-22.6 ($\underline{C}H_2CH_2COO^-$, $CH_3(\underline{C}H_2)_x$), 14.1 ($\underline{C}H_3CH_2$). IR (KBr): 3200 (b), 2922, 2851, 2150, 1648, 1551, 1436, 1376 cm^{-1}

G1(C_{14}) (as example of the series G1(C_m))

^{1}H-RMN (400 MHz, $CDCl_3$): δ= 8.50-8.30 ($CON\underline{H}$), 6.60-6.40 ($N\underline{H}^+CH_2CH_2N$, $NHCH_2CH_2N\underline{H}_3^+$, $NHCH_2CH_2N\underline{H}^+$), 3.55-3.40 ($NHC\underline{H}_2CH_2NH^+$, $NHC\underline{H}_2CH_2NH_3^+$), 3.30-3.15 ($NHC\underline{H}_2CH_2N$, $NHCH_2C\underline{H}_2NH^+$, $NH^+C\underline{H}_2CH_2CONH$, $NH^+C\underline{H}_2CH_2N$), 3.10-3.00 ($NHCH_2C\underline{H}_2NH_3^+$), 2.79-2.76 ($NC\underline{H}_2CH_2CONH$), 2.75-2.65 ($NH^+CH_2C\underline{H}_2CONH$), 2.61-2.50 ($NH^+CH_2C\underline{H}_2N$, $NCH_2C\underline{H}_2N$, $NHCH_2C\underline{H}_2N$), 2.40-2.36 ($NCH_2C\underline{H}_2CONH$), 2.34-2.28 ($CH_2C\underline{H}_2COO^-$), 1.65-1.56 ($C\underline{H}_2CH_2COO^-$), 1.32-1.24 ($CH_3(C\underline{H}_2)_x$), 0.90-0.84 ($C\underline{H}_3CH_2$). ^{13}C-RMN (400 MHz, $CDCl_3$): δ= 180.5 ($\underline{C}OO^-$), 173.6-173.0 ($\underline{C}ONH$), 52.8 ($NHCH_2\underline{C}H_2N$), 51.3 ($NH^+CH_2\underline{C}H_2N$, $NCH_2\underline{C}H_2N$), 50.2 ($N\underline{C}H_2CH_2CONH$), 44.1 ($NH^+\underline{C}H_2CH_2CONH$), 39.5 ($NHCH_2\underline{C}H_2NH^+$, $NHCH_2\underline{C}H_2NH_3^+$), 38.9 ($NH\underline{C}H_2CH_2N$), 37.3 ($NH^+\underline{C}H_2CH_2N$), 37.2 ($NH\underline{C}H_2CH_2NH^+$, $NH\underline{C}H_2CH_2NH_3^+$), 36.7 ($C\underline{H}_2COO^-$), 33.7 ($NCH_2\underline{C}H_2CONH$), 32.1 ($NH^+CH_2\underline{C}H_2CONH$), 31.9-22.6 ($\underline{C}H_2CH_2COO^-$, $CH_3(\underline{C}H_2)_x$)), 14.1 ($\underline{C}H_3$). IR (KBr): 3250 (b), 2921, 2852, 2150, 1644, 1551, 1462, 1398 cm^{-1}

G2(C_{10}): (as example of the series G2(C_m))

^{1}H-RMN (400 MHz, $CDCl_3$): δ= 8.76-8.30 ($CON\underline{H}$), 6.60-6.00 ($N\underline{H}^+CH_2CH_2N$, $NHCH_2CH_2N\underline{H}_3^+$, $NHCH_2CH_2N\underline{H}^+$), 3.51-3.40 ($NHC\underline{H}_2CH_2NH_3^+$, $NHC\underline{H}_2CH_2NH^+$), 3.32-3.28 ($NHCH_2C\underline{H}_2NH^+$), 3.26-3.24 ($NHC\underline{H}_2CH_2N$), 3.19-3.16 ($NH^+C\underline{H}_2CH_2CONH$, $NCH_2C\underline{H}_2NH^+$), 3.09-3.06 ($NHCH_2C\underline{H}_2NH_3^+$), 2.78-2.74 ($NC\underline{H}_2CH_2CONH$), 2.66-2.62 ($NH^+CH_2C\underline{H}_2CONH$), 2.58-2.55 ($NHCH_2C\underline{H}_2N$, $NCH_2C\underline{H}_2N$, $NC\underline{H}_2CH_2NH^+$), 2.40-2.36 ($NCH_2C\underline{H}_2CONH$), 2.24-2.20 ($CH_2C\underline{H}_2COO^-$), 1.60-1.50 ($C\underline{H}_2CH_2COO^-$), 1.32-1.20 (m, $CH_3(C\underline{H}_2)_x$), 0.90-0.83 (m, $C\underline{H}_3CH_2$). ^{13}C-RMN (400 MHz, $CDCl_3$): δ= 180.2 ($\underline{C}OO^-$), 174.0-171.0 ($\underline{C}ONH$), 52.0 ($NHCH_2\underline{C}H_2N$), 49.9 ($N\underline{C}H_2CH_2CONH$, $N\underline{C}H_2CH_2NH^+$), 44.0 ($NH^+C\underline{H}_2CH_2CONH$), 39.3-39.0 ($NHCH_2\underline{C}H_2NH_3^+$, $NHCH_2\underline{C}H_2NH^+$, $NCH_2\underline{C}H_2NH^+$), 37.4-37.2 ($NH\underline{C}H_2CH_2N$, $NH\underline{C}H_2CH_2NH^+$, $NH\underline{C}H_2CH_2NH_3^+$), 36.5 ($CH_2\underline{C}H_2COO^-$), 33.7 ($NCH_2\underline{C}H_2CONH$), 32.2 ($NH^+CH_2C\underline{H}_2CONH$), 31.9-22.7 ($\underline{C}H_2CH_2COO$, $CH_3(\underline{C}H_2)_x$), 14.0 ($\underline{C}H_3CH_2$). IR (KBr): 3200 (b), 2926, 2851, 2150, 1643, 1549, 1460, 1375 cm^{-1}

G3(C$_{14}$)

^{1}H-RMN (400 MHz, $CDCl_3$): δ= 8.65-8.30 ($CON\underline{H}$), 6.50-5.90 ($N\underline{H}^{+}CH_2CH_2N$, $NHCH_2CH_2N\underline{H}_3^{+}$, $NHCH_2CH_2N\underline{H}^{+}$), 3.56-3.40 ($NHC\underline{H}_2CH_2NH^{+}$, $NHC\underline{H}_2CH_2NH_3^{+}$), 3.30-3.15 ($NHCH_2C\underline{H}_2NH^{+}$, $NHC\underline{H}_2CH_2N$), 3.12-3.00 ($NH^{+}C\underline{H}_2CH_2CONH$, $NHCH_2C\underline{H}_2NH_3^{+}$, $NCH_2C\underline{H}_2NH^{+}$), 2.81-2.63 ($NH^{+}CH_2C\underline{H}_2CONH$, $NC\underline{H}_2CH_2CONH$), 2.62-2.47 ($NHCH_2C\underline{H}_2N$, $NCH_2C\underline{H}_2N$, $NC\underline{H}_2CH_2NH^{+}$), 2.45-2.30 ($NCH_2C\underline{H}_2CONH$), 2.21 ($CH_2C\underline{H}_2COO^{-}$), 1.61-1.52 ($C\underline{H}_2CH_2COO^{-}$), 1.32-1.20 ($CH_3(C\underline{H}_2)_x$), 0.89-0.85 ($C\underline{H}_3CH_2$). ^{13}C-RMN (400 MHz, $CDCl_3$): δ= 180.1 ($\underline{C}OO^{-}$), 173.8-173.2 ($\underline{C}ONH$), 52.2 ($NHCH_2\underline{C}H_2N$), 50.2 ($N\underline{C}H_2CH_2CONH$, $N\underline{C}H_2CH_2NH^{+}$), 42.3 ($NH^{+}\underline{C}H_2CH_2CONH$), 39.1-39.0 ($NHCH_2\underline{C}H_2NH^{+}$,$NHCH_2\underline{C}H_2NH_3^{+}$), 37.6-37.2 ($NH\underline{C}H_2CH_2N$, $NH\underline{C}H_2CH_2NH^{+}$, $NH\underline{C}H_2CH_2NH_3^{+}$), 36.6 ($CH_2\underline{C}H_2COO^{-}$), 34.8-34.2 ($NCH_2\underline{C}H_2CONH$, $NH^{+}CH_2\underline{C}H_2CONH$) , 31.9-22.8 ($\underline{C}H_2CH_2COO$, $CH_3(\underline{C}H_2)_x$), 14.1 ($\underline{C}H_3$). IR (KBr): 3260 (b), 2922, 2852, 2150, 1643, 1550, 1463, 1378 cm^{-1}

G4(C$_{14}$)

^{1}H-RMN (400 MHz, $CDCl_3$): δ= 8.70-8.30 ($CON\underline{H}$), 6.00-5.50 ($N\underline{H}^{+}CH_2CH_2N$, $NHCH_2CH_2N\underline{H}_3^{+}$, $NHCH_2CH_2N\underline{H}^{+}$), 3.55-3.38 ($NHC\underline{H}_2CH_2NH^{+}$, $NHC\underline{H}_2CH_2NH_3^{+}$); 3.32-3.15 ($NHCH_2C\underline{H}_2NH^{+}$, $NHC\underline{H}_2CH_2N$), 3.12-3.02 ($NH^{+}C\underline{H}_2CH_2CONH$, $NHCH_2C\underline{H}_2NH_3^{+}$, $NCH_2C\underline{H}_2NH^{+}$), 2.85-2.63 ($NH^{+}CH_2C\underline{H}_2CONH$, $NC\underline{H}_2CH_2CONH$), 2.62-2.45 ($NHCH_2C\underline{H}_2N$, $NCH_2C\underline{H}_2$, $NC\underline{H}_2CH_2NH^{+}$), 2.45-2.27 ($NCH_2C\underline{H}_2CONH$), 2.21-2.18 ($CH_2C\underline{H}_2COO^{-}$), 1.60-1.50 ($C\underline{H}_2CH_2COO^{-}$), 1.31-1.15 ($CH_3(C\underline{H}_2)_x$), 0.90-0.83 ($C\underline{H}_3CH_2$). ^{13}C-RMN (400 MHz, $CDCl_3$): δ= 180.2 ($\underline{C}OO^{-}$), 174.0 ($CONH$), 52.2 ($NHCH_2\underline{C}H_2N$), 50.1 ($N\underline{C}H_2CH_2CONH$, $N\underline{C}H_2CH_2NH^{+}$), 43.6 ($NH^{+}\underline{C}H_2CH_2CONH$), 39.2 ($NHCH_2\underline{C}H_2NH^{+}$, $NHCH_2\underline{C}H_2NH_3^{+}$, $NCH_2\underline{C}H_2NH^{+}$), 37.5 ($NH\underline{C}H_2CH_2N$, $NH\underline{C}H_2CH_2NH^{+}$, $NH\underline{C}H_2CH_2NH_3^{+}$), 36.4 ($CH_2\underline{C}H_2COO^{-}$), 35.0-33.9 ($NCH_2\underline{C}H_2CONH$, $NH^{+}CH_2CH_2CONH$) , 31.9-22.7 ($\underline{C}H_2CH_2COO$, $CH_3(\underline{C}H_2)_x$), 14.1 ($\underline{C}H_3$). IR (KBr): 3300 (b), 2922, 2852, 2150, 1644, 1551, 1463, 1376 cm^{-1}

2. Termogravimetric data.

Compound	**T_{onset}[a]**	**$T_{5\%}$[b]**
G0(C_{12})	193	156
G0(C_{14})	193	155
G0(C_{16})	205	163
G0(C_{18})	226	177
G1(C_{12})	168	148
G1(C_{14})	193	163
G1(C_{16})	195	172
G1(C_{18})	208	183
G2(C_{6})	144	138
G2(C_{8})	142	119
G2(C_{10})	151	133
G2(C_{12})	180	154
G2(C_{14})	212	170
G2(C_{16})	205	164
G2(C_{18})	219	170
G3(C_{14})	203	170
G4(C_{14})	196	166

Table S1. TGA data of the dendrimers. [a] Onset temperature of the decomposition. [b] Temperature (ºC) at which 5% of the initial mass is lost.

3. POM textures of the compounds.

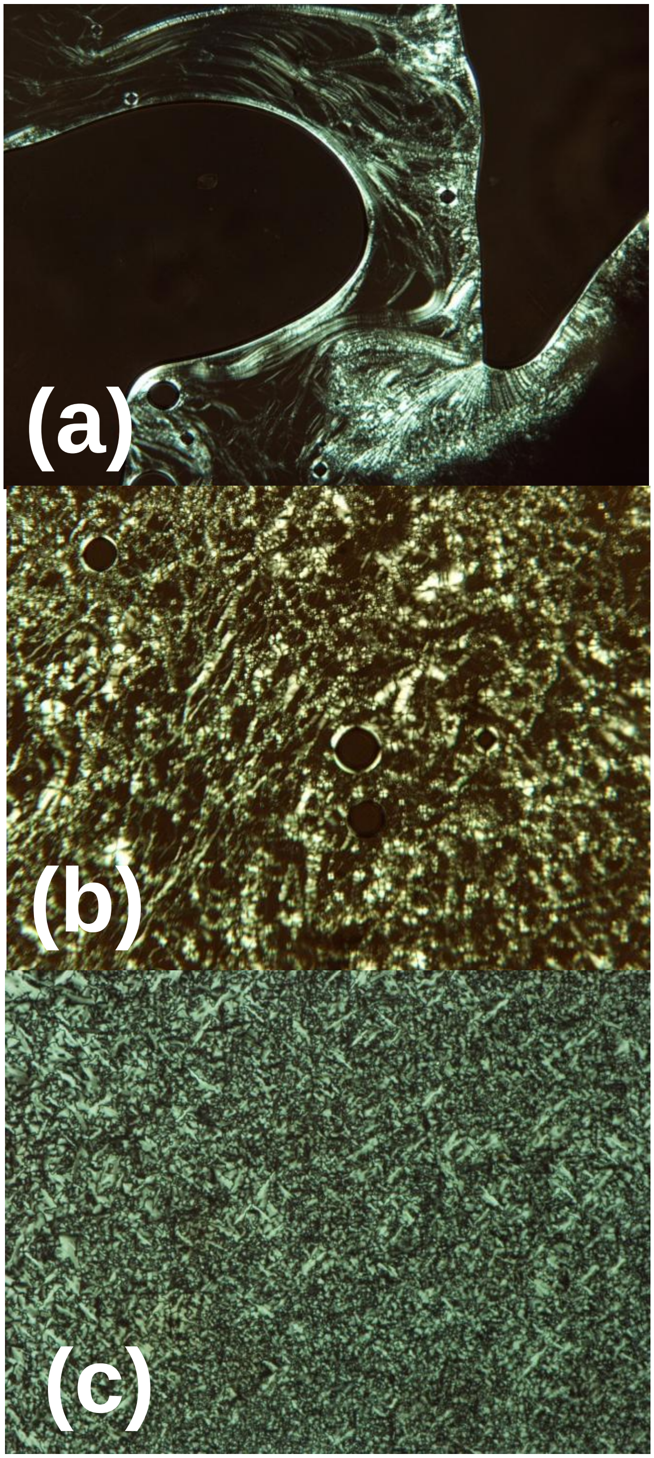

Figure S1. POM textures of a) G0(C_{12}) at 90ºC in the first heating process. b) G2(C_{12}) at 73ºC in the first heating process. c) G4(C_{14}) at 39ºC in the first cooling process.

4. Phase transition temperatures

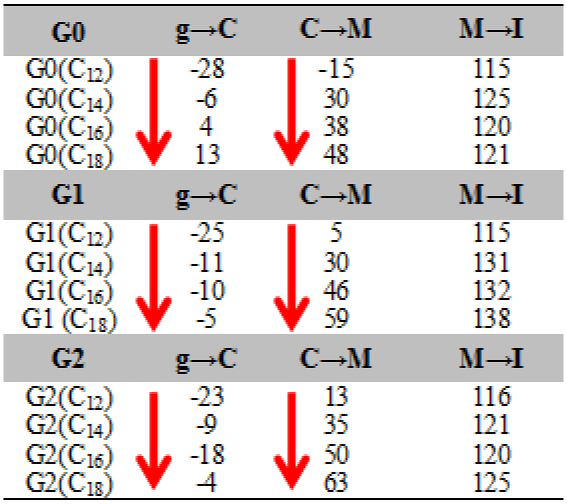

G0	g→C	C→M	M→I
G0(C$_{12}$)	-28	-15	115
G0(C$_{14}$)	-6	30	125
G0(C$_{16}$)	4	38	120
G0(C$_{18}$)	13	48	121
G1	**g→C**	**C→M**	**M→I**
G1(C$_{12}$)	-25	5	115
G1(C$_{14}$)	-11	30	131
G1(C$_{16}$)	-10	46	132
G1 (C$_{18}$)	-5	59	138
G2	**g→C**	**C→M**	**M→I**
G2(C$_{12}$)	-23	13	116
G2(C$_{14}$)	-9	35	121
G2(C$_{16}$)	-18	50	120
G2(C$_{18}$)	-4	63	125

(a)

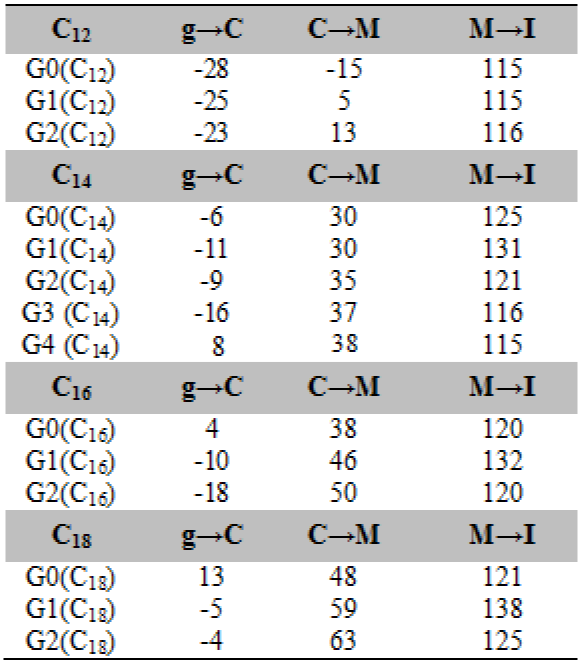

C$_{12}$	g→C	C→M	M→I
G0(C$_{12}$)	-28	-15	115
G1(C$_{12}$)	-25	5	115
G2(C$_{12}$)	-23	13	116
C$_{14}$	**g→C**	**C→M**	**M→I**
G0(C$_{14}$)	-6	30	125
G1(C$_{14}$)	-11	30	131
G2(C$_{14}$)	-9	35	121
G3 (C$_{14}$)	-16	37	116
G4 (C$_{14}$)	8	38	115
C$_{16}$	**g→C**	**C→M**	**M→I**
G0(C$_{16}$)	4	38	120
G1(C$_{16}$)	-10	46	132
G2(C$_{16}$)	-18	50	120
C$_{18}$	**g→C**	**C→M**	**M→I**
G0(C$_{18}$)	13	48	121
G1(C$_{18}$)	-5	59	138
G2(C$_{18}$)	-4	63	125

(b)

Table S2. a) Variation of the phase transition temperatures versus the length of the acid. Red arrows indicate the progressive increase in the glass and melting transition temperature with the length of the acid. b) Variation of the phase transition temperatures versus the generation of the dendrimer.

5. X-ray data

5.1. Structural parameters of the rectangular columnar mesophase.

d_{meas} (Å)	d_{calc} (Å)	*h k l*	Lattice constants (Å)
45.8	45.69	1 1 0	*a*= 74.8 *b*= 57.7
37.4	37.40	2 0 0	
26.8	26.91	1 2 0	
22.9	22.89 22.84	3 1 0 2 2 0	
4.5 (diff.)			

Table S3. X-ray results for compound G4(C_{14}) at 45ºC. d_{meas} and d_{cal} are, respectively, the measured and calculated spacing; *h k l* are Miller indexes; *a, b* are the rectangular lattice constants; *diff.* means diffuse scattering.

5.2. X-ray diffractogrammes

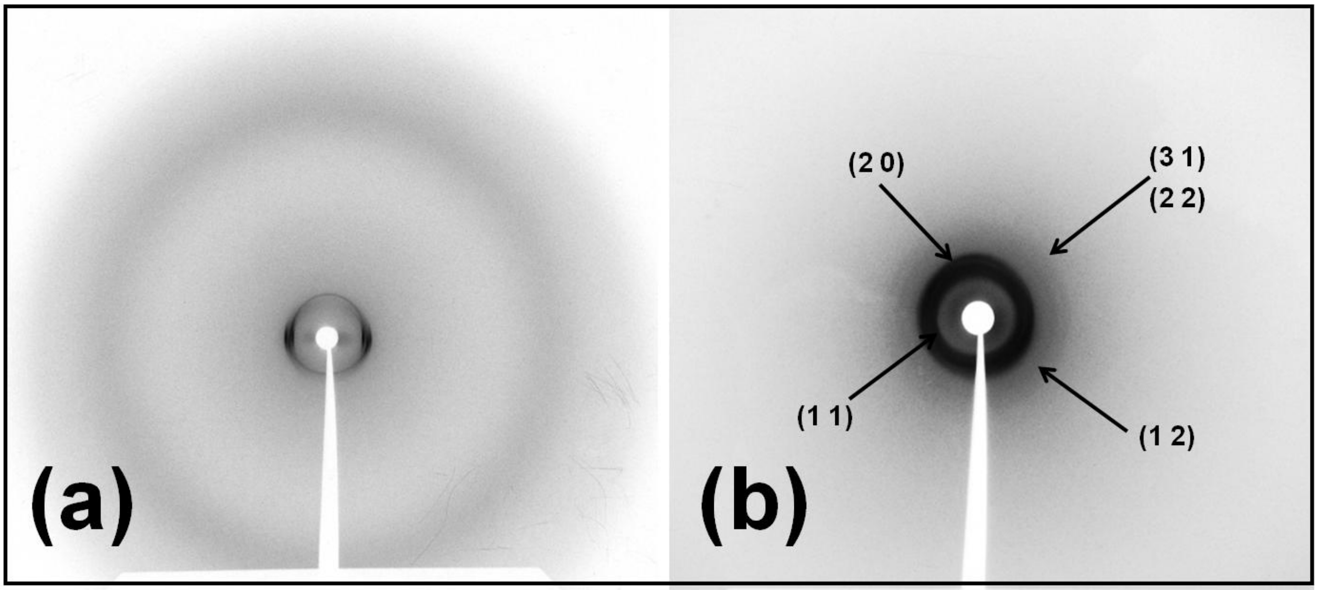

Figure S2. Small-angle XRD patterns of (a) G2(C_{10}) in the SmA phase at room temperature , (b) G4(C_{14}) in the rectangular columnar phase at 45ºC.

6. Turbidity curves by water addition.

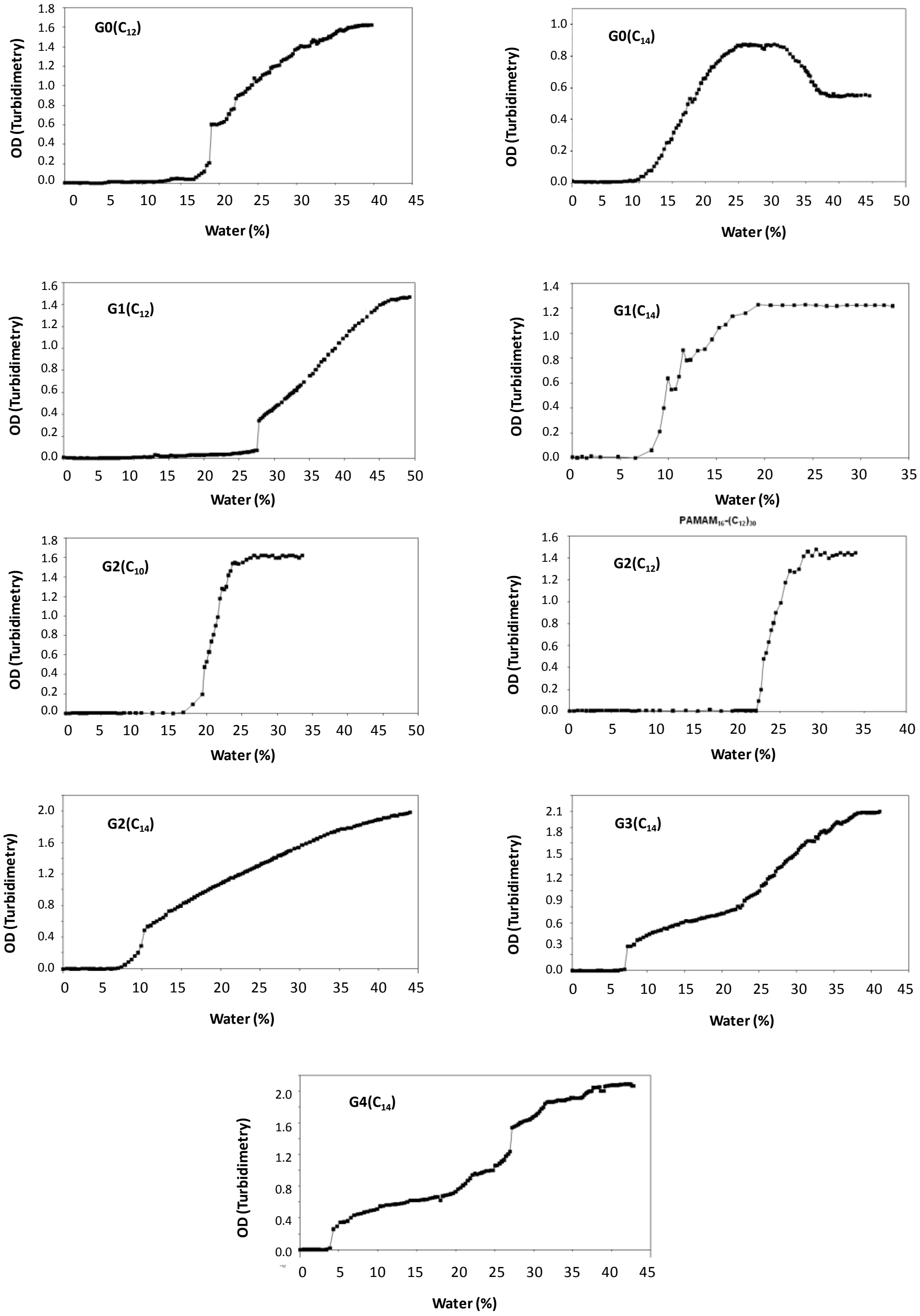

Figure S3. Turbidity (optical density) curves of the compounds in DMSO solution of (0.5%, w/w) as a function of the amount of water added to the solution

7. AFM images

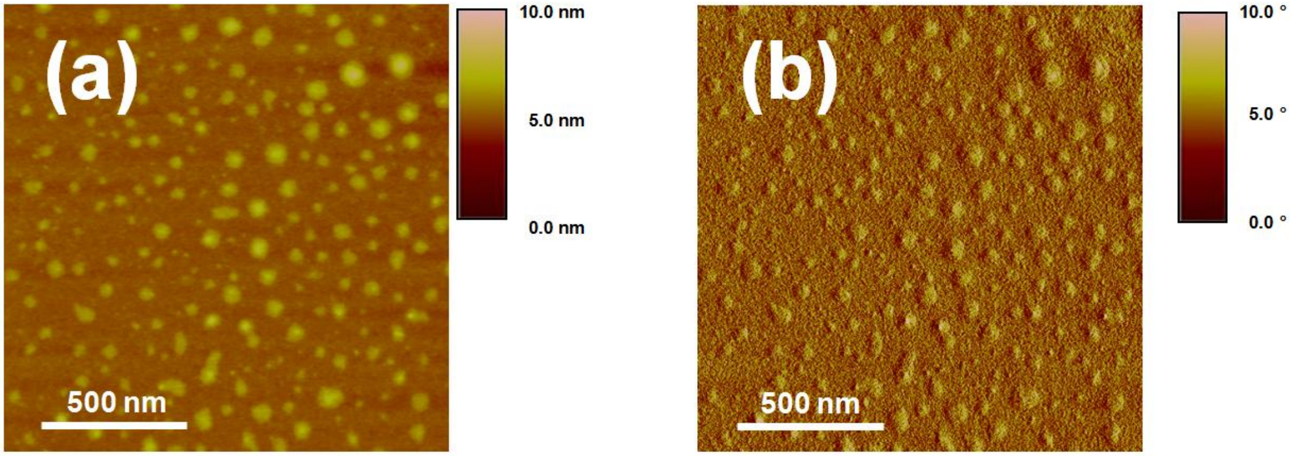

Figure S4. AFM images of G3(C_{14}) (a) topographic image, and (b) phase image.

8. TEM images

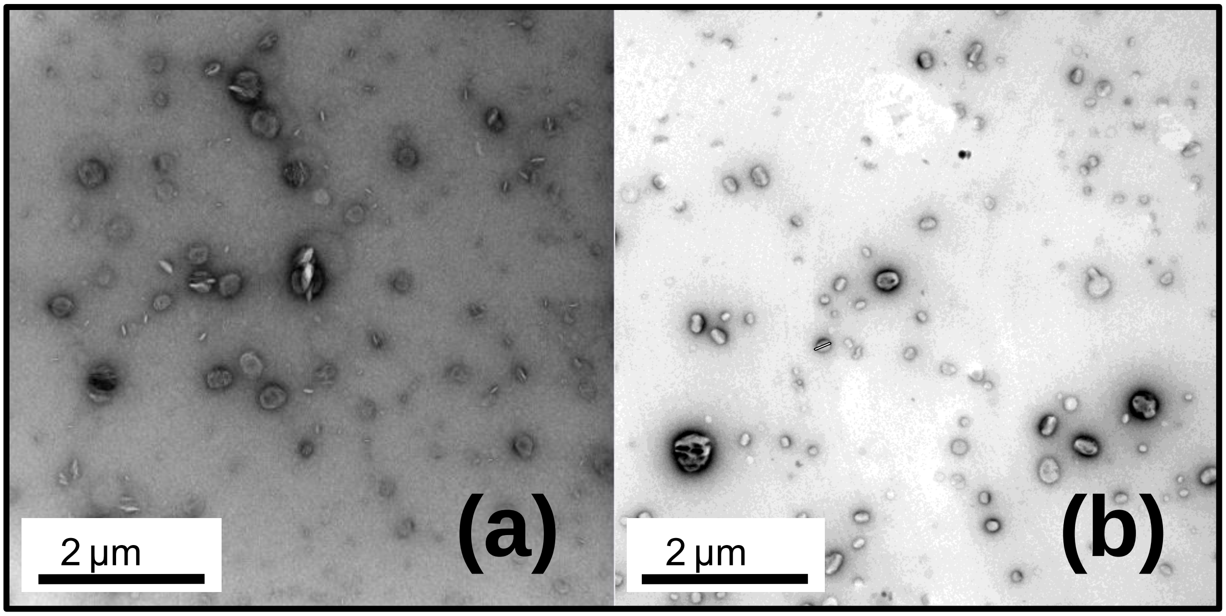

Figure S5. Representative TEM images of samples stained with uranyl-acetate. (a) G2(C_{14}) and (b) G3(C_{14})

9. Rhodamine B and β-carotene encapsulation procedures

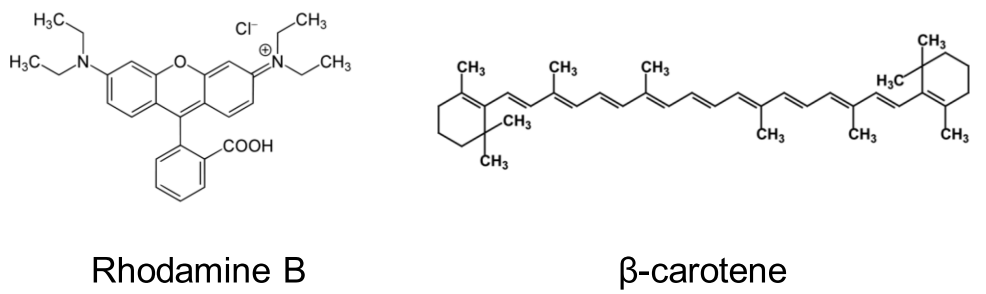

Figure S6. Chemical structure of Rhodamine B and β-carotene

Encapsulation of Rhodamine B.

0.5 mL of a solution of Rhodamine B in miliQ water was added dropwise to 0.5 ml of a solution of the G3(C_{14}) dendrimer (0.5% w/w) in DMSO. The apparition of turbidity reveals the formation of the aggregates. Then, 1 mL of miliQ water was added to the turbid solution and it was dialysed against water for one week to remove DMSO and to evaluate the percentage of non-trapped rhodamine B in the nanosphere. The absorbance of the dialysate was measured at 552 nm (λ_{max} absorption of rhodamine B in water). Measured absorptions were compared with a calibration curve of the rhodamine B previously obtained, what allowed to determine the quantity of dye molecules in the dialysate and therefore the number of molecules encapsulated in the nanosphere.

Encapsulation of β-carotene.

50 μL of a solution of β-carotene in dicloromethane was added to 0.5 ml of the solution of G3(C14) (0.5% w/w) in DMSO. After being vigorously shaked, 1 mL of desionized water was slowly added. The apparition of turbidity was observed again what indicates the presence of aggregates. To evaluate the ability of encapsulate the hydrophobic dye, this turbid solution was extracted with 1 ml of dicloromethane several times till not color was observed in the organic phase. The UV absorption of the β-carotene dicloromethane solutions was taken at 462 nm (λ_{max} absorption of β-carotene in dichloromethane). By using the calibration curve of the β-carotene previously obtained it is possible to estimate the quantity of β-carotene trapped.